*Journal of Applied Electrochemistry* **32**: 1383–1390, 2002.



# Design, construction and operation of a laboratory scale electrolytic cell for sodium production using a $\beta''$-alumina based low-temperature process

K.S. MOHANDAS[1,*], N. SANIL[1] and P. RODRIGUEZ[2]
[1]*Materials Chemistry Division, Indira Gandhi Centre for Atomic Research, Kalpakkam 603 102, India;*
[2]*Recruitment and Assessment Centre, DRDO, New Delhi 110 005, India;*
*(*author for correspondence, fax: +91 4114 480065, e-mail: ksmd@igcar.ernet.in)*

Received 7 May 2002; accepted in revised form 20 August 2002

*Key words:* beta-alumina, electrolysis, graphite/RVC anode, sodium production, sodium tetrachloroaluminate

**Abstract**

Sodium metal can be produced at low temperatures (~523 K) by electrolysis of sodium tetrachloroaluminate ($NaAlCl_4$) in a cell, which employs sodium ion conducting beta-alumina as diaphragm. A laboratory-scale electrolytic cell and associated systems were designed and constructed to study the various aspects of the energy efficient process. Graphite/reticulated vitreous carbon (RVC) was used as the anode and molten sodium as the cathode. Electrolysis was carried out at ~523 K with currents in the range 1–10 A (10–125 mA $cm^{-2}$). The cathodic current efficiency was close to 100%, but the anodic current efficiency was very low (20–30%), probably due to the consumption of chlorine in the intercalation reaction of graphite and aluminium chloride. The sodium metal was analysed by AAS and found to have 5N purity. On prolonged electrolysis, the graphite anode disintegrated due to the formation of 'graphite intercalation compounds'. RVC behaved as a better chlorine-evolving anode in the initial period of electrolysis, but its ability for chlorine evolution decreased on continuous electrolysis. The study indicated the need for effective stirring of the electrolyte with excess NaCl to avoid build up of aluminium chloride and the resultant complications in the cell.

## 1. Introduction

Sodium metal finds large-scale use in the production and storage of energy, in addition to its conventional use in the chemical and pharmaceutical industries. For example, liquid sodium is used as coolant in fast breeder nuclear reactors and as the anode in high-temperature sodium batteries. Availability of high-purity sodium at low cost is important for the economical operation of such energy systems. Industrially, sodium metal is produced by the Downs process [1–4], where sodium chloride is electrolysed at about 873 K in a fused electrolyte bath of sodium chloride and calcium chloride. The process is energy intensive on account of the high temperature melting of the electrolyte (~858 K) and also due to the inherent electrochemical characteristics of the cell. The low melting sodium compounds like sodium polysulfides, sodium tetrachloroaluminate ($NaAlCl_4$), sodium hydroxide or mixtures like NaCl–$ZnCl_2$ etc. are reactive to sodium and hence cannot be used as electrolyte in Downs cells. However, such electrolytes can be used for sodium metal production when sodium ion conducting beta alumina solid electrolyte (BASE) membrane is employed as diaphragm between the sodium metal and the molten electrolyte in the cell [5–8]. The use of the solid electrolyte membrane gives the process high current and energy efficiencies. Also the purity of the sodium metal produced by the process is exceptionally high. In spite of these advantages, the process has not been developed to the level of commercial exploitation for want of good quality beta-alumina membranes with long service life [4]. In the backdrop of the present development of secondary sodium batteries and the technological advances made in the preparation and fabrication of beta-alumina membranes, it is expected that solid electrolyte membranes suitable for sodium production will be available at affordable cost in the future.

The present study was taken up in the context of large-scale use of high-purity sodium metal as coolant in fast breeder nuclear reactors. Molten $NaAlCl_4$ was selected as the electrolyte due to its low melting point (425 K) and availability of a few patents [1–3] on the sodium production process with this electrolyte. However, no experimental data pertaining to the electrochemical characteristics of such a cell or its design aspects are available in the open literature. Hence it was the objective of this study to develop a better understanding of these aspects of the process as well as to gain experience in handling of molten chloroaluminate and sodium in a miniscale engineering facility. Ito et al. [9, 10] have reported an experimental study of the low

temperature electrolysis (623 K) of sodium chloride using a beta-alumina–molten NaCl–$ZnCl_2$ system.

### 1.1. *Process*

Direct electrolysis of NaCl–$AlCl_3$ mixtures in a cell, C|NaCl–$AlCl_3$|Al, yields aluminium metal as the cathodic product by the reaction $AlCl_4^- \rightarrow Al + 4Cl^-$. Sodium is not the cathodic product as the discharge potential of sodium ions is very negative (by $\sim$2 V) compared to that of the above reaction. However, if NaCl–$AlCl_3$ mixtures is electrolysed in a cell having the configuration, C|NaCl–$AlCl_3$|$Na^+$-ion conducting solid electrolyte/Na, sodium metal will be the cathodic product as the diaphram is selective to $Na^+$-ions.

In the present sodium production process, $\beta''$-alumina is used as the sodium ion conducting diaphragm in the two-compartment cell. Graphite in contact with molten $NaAlCl_4$ (with excess NaCl) on one side of the ceramic membrane is the anode. Molten sodium at the other side of the $\beta''$-alumina forms the cathode. When an appropriate electrical potential is applied with sodium as the negative electrode, the $Na^+$ ions in the molten electrolyte ($NaAlCl_4$ has ionic composition of $Na^+$ and $AlCl_4^-$) move towards the cathode compartment through the $\beta''$-alumina membrane and discharge to form sodium metal. The $AlCl_4^-$ ions discharge at the graphite anode to give rise to aluminium chloride and chlorine gas. The aluminium chloride produced at the anode combines with excess NaCl present in the melt to regenerate $NaAlCl_4$. As the $\beta''$-alumina is permeable to sodium ions only, the alkali metal collecting at the cathode is very pure. The configurations of the cell and cell reactions are as follows:

Cell $C|NaCl, NaAlCl_4|\beta''\text{-alumina}|Na$

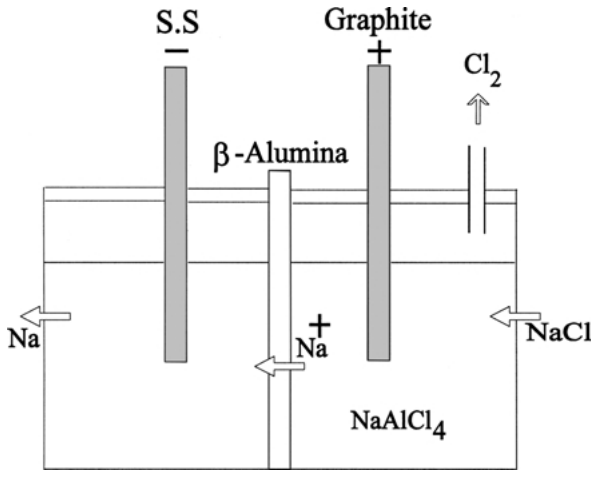


*Fig. 1.* Scheme of the low-temperature sodium production process using $\beta$-alumina separator.

Cell reactions:

$$\begin{array}{ll} AlCl_4^- \rightarrow AlCl_3 + \tfrac{1}{2}Cl_2 + e^- & \leftarrow \text{at C anode} \\ Na^+ + e^- \rightarrow Na & \leftarrow \text{at Na cathode} \\ \hline NaAlCl_4 \rightarrow Na + AlCl_3 + \tfrac{1}{2}Cl_{2(g)} & \\ AlCl_3 + NaCl \rightarrow NaAlCl_4 & \\ \hline NaCl(s) \rightarrow Na\ (l) + \tfrac{1}{2}Cl_{2(g)} & (1) \end{array}$$

The scheme of sodium production is depicted in Figure 1. A similar process with a consumable aluminium anode has been patented [7]. It is clear from the above equations that NaCl must be present in excess to regenerate $NaAlCl_4$ electrolyte necessary for continuous electrolysis. Otherwise $NaAlCl_4$ will become depleted with build up of volatile aluminium chloride in the anode compartment.

## 2. Experimental details

### 2.1. *Cell design*

#### 2.1.1. *Safety considerations*

The sodium metal and $NaAlCl_4$ electrolyte are extremely reactive to moisture and oxygen. These chemicals, separated by the beta-alumina ceramic in the cell, are also exothermically reactive to each other. In the event of failure of the ceramic membrane, the chemicals can mix together with the evolution of a large amount of heat. These concerns necessitated a cell design, which allows a minimum amount of sodium metal in the cell at any time and a mechanism for easy draining of the molten electrolyte in case of diaphragm failure. The highly volatile aluminium chloride produced during electrolysis can result in the build up of reactor pressure and in an increase of the resistivity of the melt. For these reasons, the aluminium chloride needs neutralization with excess sodium chloride. The flushing of the cell with purified argon keeps it moisture-free and also helps to reduce the pressure build-up in the reactor vessel.

#### 2.1.2. *Design of the electrochemical reactor*

The electrolytic cell is depicted in Figure 2. The cylindrical shaped cell is made of mild steel (190 mm dia. $\times$ 200 mm long $\times$ 3 mm thick) and houses a sodium-$\beta''$-alumina tube (50 mm o.d., 1.5 mm thick, 100 mm long, supplied by National Physical Laboratory, New Delhi) closed at one end. The tube with its open end downwards is fixed on the cell vessel using its $\alpha$-alumina collar. A stainless steel assembly positioned inside the $\beta''$-alumina tube serves as the cathode (sodium) current collector as well as sodium outlet. Two types of anode, one compacted graphite and the other reticulated vitreous carbon (RVC), were used in this study. The hollow-cylindrical shaped graphite anode (70 mm o.d. $\times$ 60 mm i.d. $\times$ 150 mm long) was machined from a graphite rod. The flexible RVC

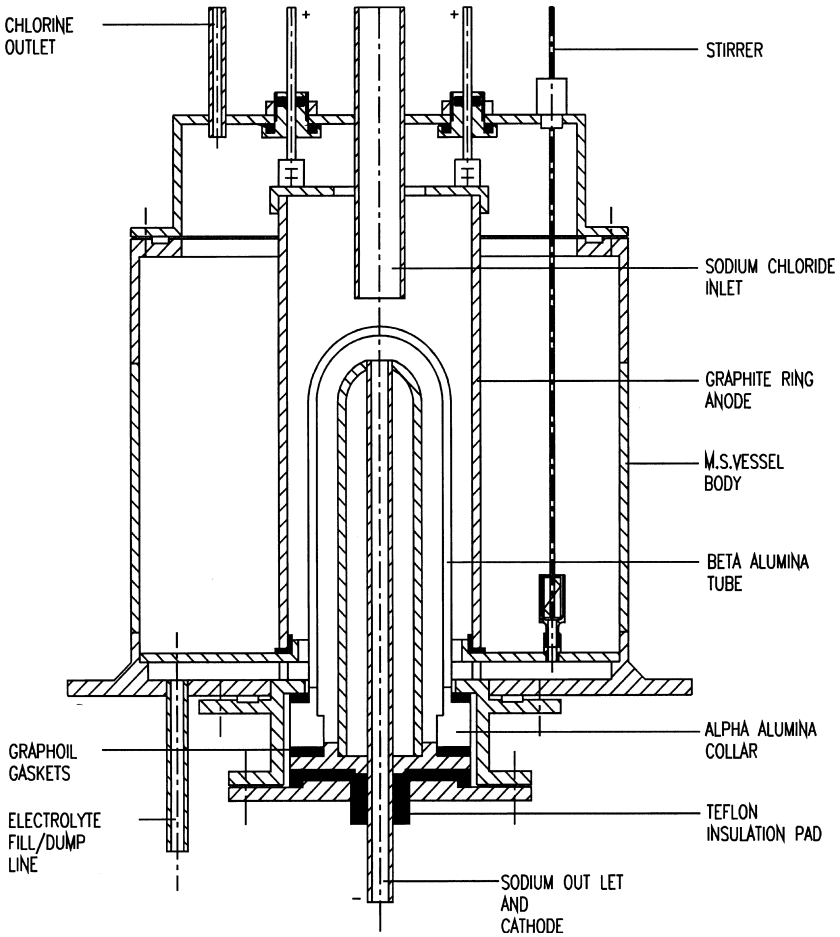


*Fig. 2.* Cross-sectional view of the electrolysis cell. The $\beta$-alumina tube is positioned at the centre of the cell with its open end downwards.

electrode of more or less similar dimension was supported in a perforated glass frame. The anode was placed around the $\beta''$-alumina tube so that the radial distance between the two was 0.5 cm. The funnel assembly provided on the cell flange was used to add sodium chloride to the cell under leak-tight conditions. Two spark-plug type level detectors were provided to monitor the level of the liquid in the reactor vessel. Provisions were made to flush argon gas over the melt in the cell as well as to stir it with bubbling argon through it. The electrolyte fill/dump line provided on the bottom of the cell allowed filling of molten electrolyte from the storage vessel to the reactor vessel and its dumping back. The flow sheet is given in Figure 3.

2.1.3. *Design of auxiliary systems*

A stream of argon gas swept the chlorine gas and aluminium chloride vapours over the melt and carried it through a moisture trap and finally to a 'chlorine absorption unit', where chlorine gas was neutralised by reaction with 15% aqueous sodium hydroxide solution (Figure 3). Apart from the chlorine absorption unit, a 'chlorine sampling unit' was also connected in parallel from the chlorine outlet line of the cell. Like the chlorine absorption unit, this unit too consisted of an array of bottles with NaOH solution so that the gas escaping the reaction in one bottle could be trapped in the successive bottles.

The cathode steel assembly, with one end inside the $\beta''$-alumina tube, extended into a calibrated Pyrex glass vessel (sodium collection vessel), which contained thermofluid at room temperature. This vessel was provided with an argon inlet-outlet so that the collection and sampling of sodium metal was done under argon atmosphere.

Electrical tape heaters and chromel–alumel thermocouples were provided on the body of all the vessels and lines in contact with the molten electrolyte/sodium. The electrolyte temperature was measured using a stainless steel sheathed chromel–alumel thermocouple placed in the melt. Argon cover gas flow was maintained over the electrolyte melt in the different vessels with the help of a gas-manifold. The argon gas was purified by passing it through a column containing a mixture of BASF catalyst and molecular sieves.

2.2. *Assembly of the cell and operation*

The electrolyte was prepared by mixing together and heating at $\sim$473 K, appropriate quantities of sodium chloride and aluminium chloride in the storage vessel. Dried NaCl (AR grade, Merck, India) and as-received $AlCl_3$ (Fluka, 99.9%) were used.

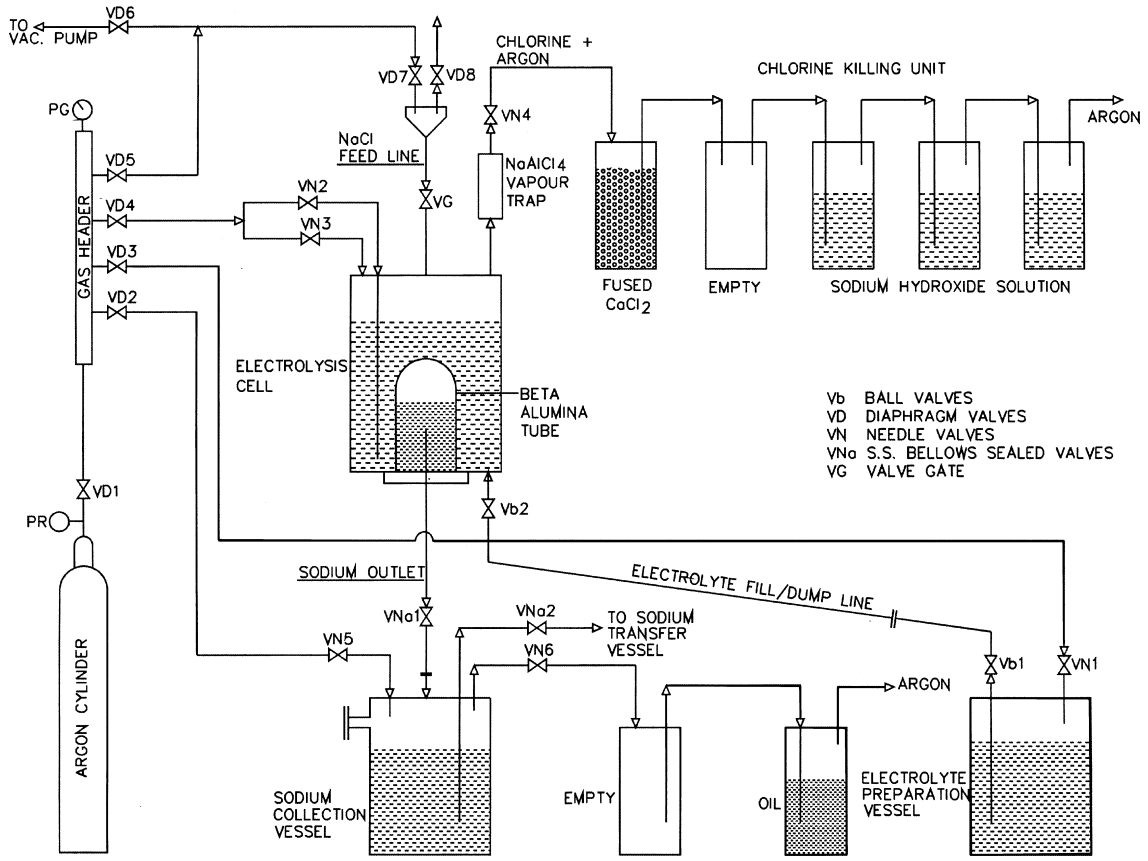


*Fig. 3.* Flow sheet of the low-temperature sodium production experiment.

Prior to use in the cells, the $\beta''$-alumina tube was etched with boiling phosphoric acid for about a minute to remove the oxide layer. Subsequently the tube was washed with alcohol and dried in air at 1073 K for ~12 h. The tube was heated overnight at 748 K with sodium metal in it to achieve sodium wetting. About 20 g of pure sodium metal was placed in the tube and the tube was fixed leak-tight to the cathode assembly with the help of 'grafoil' gaskets. The whole unit was taken out of the glove box and installed on to the bottom of the electrolysis cell vessel. The graphite and RVC anodes were degassed under vacuum at ~573 K before introduction into the cell. The entire assembly was tested for leak tightness with argon gas at 1 kg $cm^{-2}$ pressure.

With the help of the electrical tape heaters, the cell assembly was heated slowly to ~523 K. Argon gas was flushed through the entire setup for ~24 h to flush out moisture. The molten electrolyte was then transferred to the electrolytic cell by maintaining a differential pressure between the cell and the electrolyte storage vessel and following the flow sheet in Figure 3. The cell temperature was maintained in the range 498–523 K and electrolysis was carried out at currents of 1–2 A. In order to make an assessment of the cell voltage as a function of current, the current was increased in steps of 1 A to a maximum of 10 A for short times. The sodium and chlorine half cell potentials were measured using an aluminium reference electrode in NaCl saturated $NaAlCl_4$ melt, positioned close to the anode. The cell voltages were measured using a high impedance voltmeter (HP Data Acquisition/Switch unit 34970A). The voltage at zero current was obtained by manually interrupting the current during electrolysis.

The quantity of sodium metal produced by electrolysis was obtained by measuring the difference in the level of the thermofluid in the sodium collection vessel before and after sodium addition. Chlorine gas evolved over a specified time was collected in cold, aqueous NaOH solution and analysed by iodimetry.

## 3. Results and discussion

To compare the electrochemical data obtained from the cell, the cell voltage and energy efficiency of the process were estimated for a model cell having identical cell characteristics.

### 3.1. *Estimation of cell voltage and energy efficiency*

The terminal voltage of a cell, based on the dimensions of the model cell in Figure 4, was calculated using the relationship

$$E_{\text{cell}} = E_{\text{rev(NaCl)}} + E_{\beta''} + E_{\text{NaAlCl}_4} + \eta_{\text{cathode}} + \eta_{\text{anode}} + E_{\text{s}}$$

where $E_{\text{rev(NaCl)}}$ is the reversible decomposition voltage of sodium chloride, $E_{\beta''}$ the voltage drop due to resistance of the $\beta''$-alumina diaphragm, $E_{\text{NaAlCl}_4}$ the

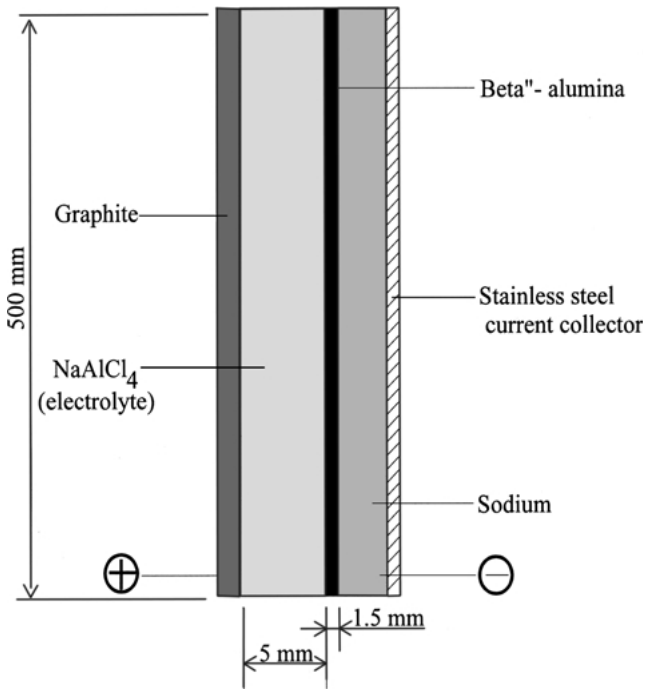


*Fig. 4.* Model cell design with beta-alumina separator.

voltage drop due to resistance of molten $NaAlCl_4$, $\eta_{cathode}$ the sodium cathode overvoltage, $\eta_{anode}$ the graphite anode overvoltage, and $E_s$ the voltage loss in the electrodes and cell hardware.

The cell voltage in turn is related to the energy efficiency of the process as

$$\text{Energy efficiency} = E_{cell}/E_{rev} \times \text{current efficiency}$$

The data available in the literature, as well as some data generated in our laboratory for the components of such a cell [11–13] were used in these calculations. Similar calculations were also carried out for a conventional Downs cell. The operational parameters of both the beta-alumina based cell and Downs cell, used in these calculations, are give in Table 1. More details of these calculations are given in elsewhere [11].

These calculations have shown that a cell voltage of 5.3 V and energy efficiency 67% could be possible for the beta-alumina based process as against 7 V and 40% for the conventional Downs process. The electrolysis energy for the two processes worked out to 6.5 kWh $kg^{-1}$ and 10.6 kWh $kg^{-1}$, respectively. The cell voltage, energy efficiency and the specific energy for sodium production estimated for the Downs process are generally in good agreement with the data reported from operating cells [1–4]. In the absence of reported data, a similar comparison is not possible for the beta-alumina based process. Typical plots of the voltage balance of the model beta-alumina cell (Figure 4) and the corresponding energy efficiency values as a function of current density are given in Figures 5 and 6, respectively.

### 3.2. *Cell voltage*

#### 3.2.1. *Graphite anode*

A typical voltage–time profile of the cell with a graphite anode during electrolysis at 1 A current at 498 K is given in Figure 7. From the working voltage of the cell (3.85 V) and the voltage on current interruption (3.79 V), the cell resistance was inferred as about 60 mΩ. The cell voltage remained more or less stable for more than 12 h and recorded a very slow increase thereafter. The cell voltages remained less than 4 V during continuous electrolysis at 1–2 A for about 50 h.

The cell voltages measured in the current range 1–10 A for short times are given in Table 2. The voltages estimated for the model cell under similar experimental conditions are also given in the table. The overvoltages due to electrode polarization are not considered in the calculation as the duration of electrolysis was too short for polarization to set in. Good agreement between the measured and estimated cell voltages are seen.

As electrolysis continued, the cell developed electrical discontinuity repeatedly. Physical examination of the cell showed that the graphite anode had disintegrated. Similar behaviour was noticed on two more fresh graphite anodes. The problem was subsequently studied using cyclic voltammetry and found to be due the formation of graphite intercalation compounds and the volume expansion that accompanies the GIC formation [14, 15]. This conclusively proved that graphite is reactive in the chloroaluminate melt and cannot be used as

*Table 1.* Characteristics of Downs cell and beta-alumina based cell for sodium production

| Purticulars | Downs process | $\beta''$-alumina process |
|---|---|---|
| Electrolyte | NaCl (41–42 wt%) + $CaCl_2$ (58–59 wt%) | NaCl (30wt%) + $AlCl_3$ (70 wt%) |
| Anode | Graphite | Graphite (?) |
| Cathode | Cast steel | Sodium |
| Inter-electrode spacing /cm | 3.7 | 0.5 |
| Electrolyte temperature /K | 863 ± 5 | 573 |
| Cell voltage /V | 6–7[a]<br>7.05[b] | 5.12[b] |
| Cathode current density /A $cm^{-2}$ | 0.98[a] | 0.5 |
| Current efficiency /% | 78–80[a] | >95[a] |
| Energy efficiency /% | 38–45[a] | >60[b] |

[a] reported, [b] calculated.

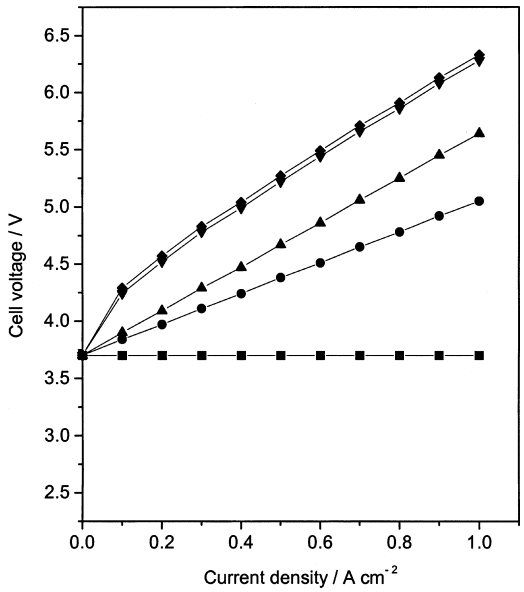


*Fig. 5.* Estimated voltage balance of the model cell as a function of current density at 573 K. (a) $E_{rev}$(NaCl), (b) $a + E_{\beta}$, (c) $b + E_{NaAlCl_4}$, (d) $c + \eta_{anode}$ and (e) $d + E_s$ where (a, b, c, d and e) are represented by (■, ●, ▲, ▼ and ◆), respectively.

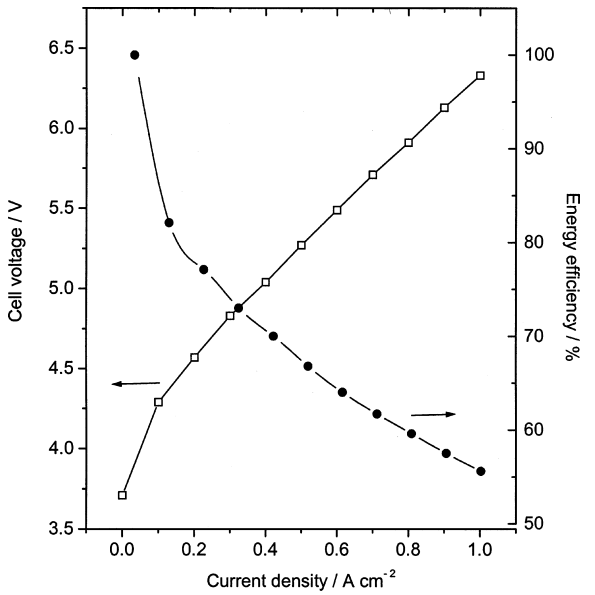


*Fig. 6.* Estimated cell voltage and energy efficiency of the model cell as a function of current density.

anode for electrolysis of chloroaluminate melt [16]. Preliminary electrochemical studies with a RVC anode showed that it is more stable in the chloroaluminate melt and hence used in the electrolysis.

### 3.2.2. *RVC anode*

The variation of the cell voltage with time during the initial phase of constant current electrolysis, under similar experimental conditions used for the graphite anode, is given in Figure 7. The overvoltage of the RVC cell was deduced as 540 mV as against 60 mV for the

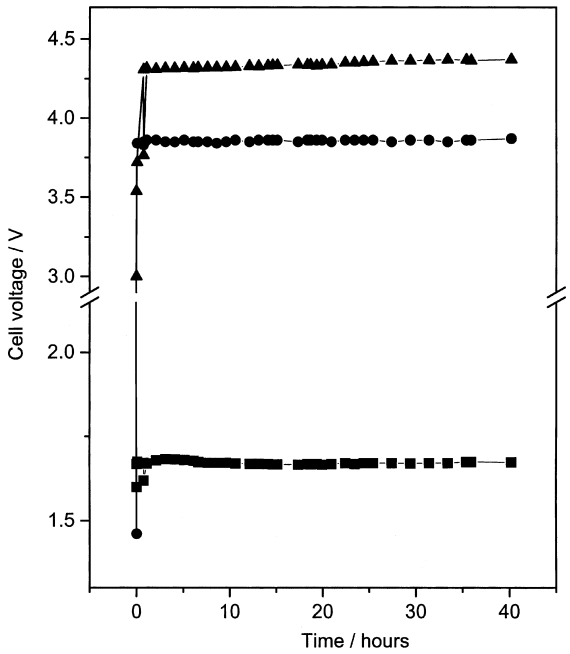


*Fig. 7.* Behaviour of cell voltages during constant current electrolysis at 498 K. Current 1 A. Key: (●) graphite anode and (▲) RVC anode. Potentials of the sodium electrode during electrolysis, measured against the Al reference electrode, are given by (■). Graphite and RVC anode potentials (vs Al) can be obtained by subtracting the Na electrode potentials from the respective cell voltages.

*Table 2.* Variation of the cell voltage of the $\beta$-alumina based cell with current density

| S.no | Current /A | Current density /mA cm$^{-2}$ of $\beta''$-alumina | Cell voltage /V | |
|---|---|---|---|---|
| | | | Measured | Estimated |
| 1 | 1.0 | 12.5 | 3.83 | 3.84 |
| 2 | 2.0 | 25.0 | 3.90 | 3.87 |
| 3 | 4.0 | 50.0 | 3.95 | 3.94 |
| 4 | 6.0 | 75.0 | 4.02 | 4.02 |
| 5 | 8.0 | 100.0 | 4.15 | 4.09 |
| 6 | 10.0 | 125.0 | 4.23 | 4.16 |

graphite cell. The higher overvoltage of the former may be attributed to the higher resistivity of RVC, which is about ten times higher than that of graphite.

The cell was operated continuously at 1–2 A (10–20 mA cm$^{-2}$) levels, for about four months with short breaks. About 2000 Ah charge was passed through the cell during this period. The current density had to be limited to very low values as effective stirring of the electrolyte could not be achieved due to the deposition of anodically generated aluminium chloride on the stirrer and on the cooler parts of the cell. With passage of time the stirrers were rendered virtually immobile and the cell had to be operated under static condition, which increased the cell voltage. It is possible that the build up of the electrolytically generated aluminium chloride in the melt, in the absence of proper mixing of with solid NaCl, increased the resistance of the melt and hence the cell voltage.

*Table 3.* Results of the determination of cathodic current efficiency of the sodium production cell

| Current /A | Duration /h | Total charge passed /Ah | Quantity of sodium /g | | Current efficiency /% |
|---|---|---|---|---|---|
| | | | Measured | Theoretical | |
| | 24 | 24 | 20.2 | 20.59 | 98.1 |
| 1 | 50 | 50 | 43.0 | 42.9 | 100 |
| | 88 | 88 | 74.4 | 75.5 | 98.5 |
| 1.5 | 28 | 42 | 35.3 | 36.04 | 97.9 |
| | 52 | 78 | 64.2 | 66.9 | 96 |
| 2 | 14 | 28 | 23.9 | 24.02 | 99.5 |
| | 24 | 48 | 40.0 | 41.19 | 97.2 |

*Table 4.* Results of the determination of the anodic current efficiency of the sodium production cell

| Current /A | Duration of electrolysis /h | Total charge passed /Ah | Quantity of chlorine /g | | Current efficiency /% |
|---|---|---|---|---|---|
| | | | Measured | Theoretical | |
| 1 | 2 | 2 | 0.70 | 2.65 | 26.4 |
| | 4 | 4 | 1.70 | 5.3 | 32 |
| 1.5 | 1.5 | 2.25 | 0.79 | 2.98 | 26.4 |
| | 2 | 3 | 1.35 | 3.97 | 34 |
| 2 | 1 | 2 | 0.77 | 2.65 | 29.2 |
| | 2.5 | 5 | 2.11 | 6.62 | 32 |

An interesting behaviour of the cell voltage was noticed on continuous electrolysis with the RVC anode. As electrolysis proceeded, the cell voltage decreased by ~400 mV compared to that at the beginning of electrolysis. An analysis of the half cell potentials revealed that the decrease in overvoltage was entirely due to the RVC anode and anodic reactions involving chlorine were responsible for it. SEM pictures of the electrode showed clear signs of deterioration and surface modification [11].

### 3.3. *Current efficiency*

From the charge passed and the quantity of sodium collected (Table 3), the current efficiency of the process was calculated to be close to 100%, within experimental error. In the absence of current leakage in the cell, it was expected that the entire current should have passed through the beta-alumina to give the current efficiency as obtained above. The results, conversely, can be taken as experimental proof that the transport number of beta-alumina (for $Na^+$-ions) is close to unity.

The results of the analysis of chlorine collected for different times and for currents of 1–2 A are given in Table 4. In contrast to the high cathodic efficiency (sodium), the anodic efficiency (chlorine) is very low. As the anode and cathode compartments are physically separated by the beta-alumina diaphragm, combination of the primary electrolytic products cannot be the reason for the low anodic current efficiency. This would suggest that a good part of the anodic chlorine was consumed in reactions involving the RVC and chloroaluminate melt. The results of cyclic voltammetric studies of carbon materials in the chloroaluminate support this [14].

*Table 5.* Comparison of the impurity levels in the sodium metal produced in the $\beta$-alumina based cell and the Downs cell

| Impurity element | Concentration /ppm | | |
|---|---|---|---|
| | $\beta''$-alumina process | Downs process | |
| | | Commercial grade | Nuclear grade /max |
| Fe | < 0.1 | – | 3.0 |
| K | 0.28 | 100–200 | 300 |
| Al | < 0.1 | 2.0 | 5.0 |
| Ca | 0.81 | 40–300 | 10 |
| Mg | 0.31 | 100 | 0.05 |

### 3.4. *Analysis of sodium*

The sodium metal collected directly from the cell using a tantalum crucible was analysed for probable impurities such as Fe, K, Al, Ca and Mg by atomic absorption spectrometry (AAS). The results are given in Table 5. A comparison shows that the purity of the sodium metal produced by the low-temperature process is better than that of the 'nuclear grade' sodium with respect to these elements. The other impurity elements such as C, Cr, B, Cd, Ag, S, Co, Pb, Mn, Ni and Zn present in trace levels in Downs cell sodium is unlikely to be present in the

sodium produced in the new process as beta-alumina diaphragm electrically filters these elements.

## 4. Conclusion

A comparative study of the beta-alumina based process and Downs process for sodium production shows that the former process is superior on account of its low electrolysis energy and high sodium purity. The limited electrochemical data generated in this work supports this. However, it should be made clear that it was not the aim of the present work to make a critical assessment of the two processes, but was only an effort to understand some of the technical problems of the low-temperature process. The safe operation of the experimental cell for a reasonably long period of time has demonstrated the validity of the cell design and the technical feasibility of the low-temperature process on the lab scale. The results categorically rule out the use of graphite as anode. But, the estimated and measured cell voltages with a graphite anode points to the fact that it may be possible to operate beta-alumina based cells with an anode of similar electrochemical characteristics, but inert towards chlorine. New generation chlorine-evolving anodes like the titanium substrate insoluble anode (TSIA) or ceramic oxide/glassy carbon coated graphite may prove to be better anodes. Due to the high resistivity, RVC may not be an ideal anode. The build up of aluminium chloride in the cell and the resultant blockage of inlet–outlet pathways of the reactor vessel are identified as the most serious problems. This observation underlined the need for proper mixing of the electrolyte with excess sodium chloride and a cell design which can prevent the deposition of aluminium chloride on the cooler parts of the cell. This may be better achieved with a cell in which the electrolyte melt saturated with NaCl is pumped from outside and flows continuously around the beta-alumina diaphragm. Such a design will make the operation of the cell less complicated and will give a better diaphragm service life.

## References


1. M. Sittig, 'Sodium: Its Manufacture, Properties and Uses' (Reinhold Publishing Corporation, New York, 1956), pp. 10–44.
2. A.T. Kuhn, 'Industrial Electrochemical Processes' (Elsevier, Netherlands, 1971), p. 99.
3. Mellor's 'Comprehensive Treatise on Inorganic and Theoretical Chemistry', Vol. II, Supplement II, The alkali metals, Part I (Longman, 1961), pp. 323–325.
4. C.H. Lemke, Sodium and its alloys, *in* 'Encyclopedia of Chemical Technology', **21** (Kirk Othmer, 1983), p. 193.
5. *British patent 1 200 103* (1967).
6. *British patent 1 155 927* (1969).
7. *British patent 2 193 226* (1988).
8. K.S. Mohandas, 'Beta-alumina Based Process for Sodium Manufacture', Report IGC-160 (1994).
9. Y. Ito, S. Yoshizawa and S. Nakamatsu, *J. Appl. Electrochem.* **6** (1976) 361.
10. H. Hayashi, S. Nakamatsu and Y. Ito, *J. Appl. Electrochem.* **15** (1985) 225.
11. K.S. Mohandas, PhD thesis, University of Madras, Jan. (2001).
12. K.S. Mohandas, N. Sanil, Tom Mathews and P. Rodriguez, *Metall. Mater. Trans.* **32B** (2001) 669.
13. K.S. Mohandas, N. Sanil and P. Rodriguez, *in* Proceedings of the National Symposium on 'Electrochemistry in Nuclear Technology' (Kalpakkam 1998), pp. 157–162.
14. K.S. Mohandas, N. Sanil, M. Noel and P. Rodriguez, *J. Appl. Electrochem.* **31** (2001) 997.
15. H. Wendt, A. Khalil and C.E. Padberg, *J. Appl. Electrochem.* **21** (1991) 929.
16. K.S. Mohandas, N. Sanil and P. Rodriguez, *in* Proceedings, *op. cit.* [13], pp. 163–168.